



**HAL**  
open science

# Low-loss Magnetodielectric Spinel-ferrite Based Ceramic with Constant Permeability and Permittivity in the UHF Range

Atul Thakur, Jean-Luc Mattei, Alexis Chevalier, Patrick Queffelec

► **To cite this version:**

Atul Thakur, Jean-Luc Mattei, Alexis Chevalier, Patrick Queffelec. Low-loss Magnetodielectric Spinel-ferrite Based Ceramic with Constant Permeability and Permittivity in the UHF Range. IEEE International Conference on Ferrites, May 2009, Sacramento, United States. pp.BF-09. hal-00489017

**HAL Id: hal-00489017**

**<https://hal.univ-brest.fr/hal-00489017>**

Submitted on 14 Jun 2010

**HAL** is a multi-disciplinary open access archive for the deposit and dissemination of scientific research documents, whether they are published or not. The documents may come from teaching and research institutions in France or abroad, or from public or private research centers.

L'archive ouverte pluridisciplinaire **HAL**, est destinée au dépôt et à la diffusion de documents scientifiques de niveau recherche, publiés ou non, émanant des établissements d'enseignement et de recherche français ou étrangers, des laboratoires publics ou privés.

# Low-loss Magnetodielectric Spinel-ferrite Based Ceramic with Constant Permeability and Permittivity in the UHF Range

A. Thakur, A. Chevalier, J.-L. Mattei, and P. Queffelec, *Senior Member, IEEE*

Laboratoire des Sciences et Techniques, de l'Information, de la Communication et de la Connaissance,  
Lab-STICC-UMR CNRS 3192, 6 av. Le Gorgeu, CS 93837, 29238 BREST CEDEX 3, France.

**Ni-Co-Zn nanoparticles of composition  $\text{Ni}_{0.5}\text{Zn}_{0.3}\text{Co}_{0.2}\text{Fe}_2\text{O}_4$  were successfully prepared by co-precipitation method. After sintering the average grains size is about 100nm. The material obtained after adequate heat treatment lies between ceramic (with porosity equal to 15%) and composite medium. It shows almost constant complex permeability and permittivity in the frequency range from 100MHz to 1 GHz, and equal to  $\sim 3.5-j0.15$  (loss tangent $\sim 0.04$ ) and  $\sim 6-j0.13$  (loss tangent $\sim 0.02$ ) respectively. The refractive index  $n$  is close to 4.85. Relaxation phenomenon takes place at 2.34 GHz, an unusual value for spinel ferrites. These electromagnetic properties, in particular the low levels of losses, show that this material could be useful to the design of miniaturized antennas in the VHF-UHF (30MHz-500MHz) range of frequency.**

**Index Terms**—Electromagnetic measurements, Magnetic losses, Magneto-dielectric material for miniaturized antenna, Microwave ferrites.

## I. INTRODUCTION

WITH the present rapid growth in terrestrial and satellite communications, a myriad of applications are envisioned for microwave devices of reduced size. In particular, the tremendous development of handheld terminals in the UHF range asks for antennas of reduced physical dimension without affecting their electrical performances. Actually, present antennas are too large to allow satisfactory integration into such devices, and the present techniques used to reduce their size degrade the performances of the antennas [1]. Materials with low dielectric and permeability loss tangents are very useful to the design of miniaturized antennas and simultaneously maintaining the electrical dimensions. However, information on natural low-loss materials in 100MHz to 1GHz frequency range is mainly lacking. Actually, materials that show sufficiently low magnetic and dielectric loss tangents ( $\text{tg}\delta_\mu = \mu''/\mu'$  and  $\text{tg}\delta_\epsilon = \epsilon''/\epsilon' < 10^{-2}$ ) and a refractive index ( $n = \sqrt{\mu' \epsilon'}$ ) large enough, could be useful to the design of antennas with reduced physical dimensions (where  $\mu'$  and  $\epsilon'$  are real parts of relative permeability and permittivity respectively, and  $\mu''$  and  $\epsilon''$  the imaginary parts). A criterion that is invoked sometime is that of a reduced-

impedance matched to free space ( $Z/Z_0 = \sqrt{\mu'/\epsilon'}$ , with  $\mu' =$

$\epsilon'$ ) for the substrate [2]. This constraint will be relaxed in our study, because the above criterion should be applied to the whole antenna, and not to its substrate.

Garnets are very good candidates for non-reciprocal devices (circulators, isolators) due to their low-resonance line-width, but they exhibit very low permeability values at microwave frequencies. Although Ni-Zn ferrites are useful for radiofrequency applications, i.e. up to 300MHz, it is not usual to use spinel ferrites for microwave devices, i.e. above 300MHz. For use in the microwave band, hexagonal ferrite are preferred because of their high resonance frequency (commonly higher than 3GHz). Actually, to achieve low-loss

requirement, the material must have a resonant frequency far from the desired frequency band. Our task is concerned with soft material-spinel ferrite-that would show potentiality to be used in the frequency range 300MHz-1GHz. The important task is to shift the resonance frequency of basic Ni-Zn ferrites beyond the desired frequency range by keeping low electrical and magnetic losses.

The basic composition of  $\text{Ni}_x\text{Zn}_{1-x}\text{Fe}_2\text{O}_4$  was selected because of its relative high permeability, and low magnetic loss tangent. First of all,  $\text{Ni}_{0.5}\text{Zn}_{0.5}\text{Fe}_2\text{O}_4$  was optimized from  $\text{Ni}_x\text{Zn}_{1-x}\text{Fe}_2\text{O}_4$  series for its better electromagnetic properties. Then, cobalt was substituted for zinc as  $\text{Ni}_{0.5}\text{Zn}_{0.5-y}\text{Co}_y\text{Fe}_2\text{O}_4$ , since cobalt is effective to shift resonance at higher frequency region by increasing the magnetic anisotropy [3]-[4] and finally  $\text{Ni}_{0.5}\text{Zn}_{0.3}\text{Co}_{0.2}\text{Fe}_2\text{O}_4$  was optimized. Therefore, the present study aims to investigate cobalt substituted nickel zinc spinel ferrites of nominal composition  $\text{Ni}_{0.5}\text{Zn}_{0.3}\text{Co}_{0.2}\text{Fe}_2\text{O}_4$  for electromagnetic applications in the UHF range.

## II. EXPERIMENTS

Ni-Co-Zn ferrite of composition  $\text{Ni}_{0.5}\text{Zn}_{0.3}\text{Co}_{0.2}\text{Fe}_2\text{O}_4$  was prepared via the conventional co-precipitation method [5]. The materials used were nickel chloride hexahydrate (99.9% Aldrich, Germany), cobalt chloride hexahydrate ( $\geq 98\%$  Fluka, USA), zinc chloride (99.9% Aldrich, Germany), iron (III) chloride hexahydrate (99% Riedel-de Haen, Germany) and sodium hydroxide (99% Merck, Germany). One molar solution of these materials was made with double distilled water. A quantity of 70ml sodium hydroxide was taken from one molar solution in approximately 1760ml of distilled water to get the concentration of 0.37 mol/litre and heated to boiling. Nickel chloride, cobalt chloride, zinc chloride and iron (III) chloride were taken from their molar solution in accurate stoichiometric proportions. These solutions were poured as quickly as possible into boiling solution of NaOH under vigorous stirring produced by the magnetic stirrer ( $\sim 1200$  r.p.m.). Mixing is very important otherwise segregation of phases can take place. After co-precipitation, pH is set

between 11.5-12. Reaction vessel is covered with plastic cover to diminish evaporation of the solution. Reaction is continued for 30-40 minutes at temperature 90-100°C under vigorous stirring. Reaction vessel is cooled to ambient temperature and particles precipitate. Total volume is reduced to ~500ml by aspiration of supernatant. Suspension is centrifuged at 6000 r.p.m. for 10 minutes. Precipitate is washed carefully with distilled water to remove the contents of sodium and centrifuged once more in at 6000 r.p.m. for 10 minutes. The residue is dried in an electrical oven for overnight, before to be calcinated (temperature  $T_c=800^\circ\text{C}$ ) in air for 3 hour (with heating and cooling rates of  $200^\circ\text{C/h}$ ) to obtain a ferrite powder. Then this powder was pressed into toroids under a pressure of 25MPa using uniaxial hydraulic press. These samples were sintered in air at temperature  $T_s$  for another 3 hour at a heating rate of  $200^\circ\text{C/h}$  and were subsequently cooled with the same rate to room temperature. The values of  $T_s$  chosen for the samples are shown Table 1.

### TABLE 1 HERE

## III. RESULTS AND DISCUSSION

### A. Structural studies and static permeability

Figure 1 shows the XRD pattern recorded for  $\text{Ni}_{0.5}\text{Zn}_{0.3}\text{Co}_{0.2}\text{Fe}_2\text{O}_4$  in powder form after calcination ( $T_s=800^\circ\text{C}$ ). The observed diffraction lines were found to correspond to that of single phase cubic spinel structure. Under the experimental conditions used no unreacted constituents were present in these samples. The estimated average particle size is found to be 25 nm by using Scherer's equation for Lorentzian peak [5] from the broadening of most intense peak (311). This value is confirmed by TEM observation (not shown). The lattice parameter was found to be 8.374 Å, which is in close agreement with the American Society for Testing Materials (ASTM) and with the published results for Ni-Zn ferrite obtained through other methods [7]-[8].

### FIG. 1 HERE

Figure 2 depicts SEM image of the surface of sample (a) after sintering. Due to grain growth during sintering, the average grain size is found to be about 100nm. This value is far below the critical size  $d_m$  for multi-domain grains placed in the empty space [9]. Moreover, it has been also demonstrated that  $d_m$  is increased when the single-domain grain is embedded in a magnetic environment [9].

### FIG. 2 HERE

The first magnetization curves of samples (a) and (d) has been measured using the transformer method (Fig. 3). The values of the initial susceptibilities  $\chi_{\text{init}}$  calculated from these results (see Table 1) are characteristic of spin component, and close to expected values for NiZn ferrites.

### FIG. 3a and 3b HERE

### B. Microwave characterization of complex permeability and permittivity

The material parameters  $\epsilon$  (complex permittivity  $\epsilon'-j\epsilon''$ ) and  $\mu$  (complex permeability  $\mu'-j\mu''$ ) were measured using the transmission/reflection method based on the algorithms of Nicolson, Ross and Weir for the broadband characterization of isotropic solid material and the iteration procedure from Baker-Jarvis [10]. The method is based on the measurements of the scattering parameters of a toroidal sample placed into a coaxial line. An error analysis indicates moderate uncertainties in  $\epsilon'$  (<5%),  $\epsilon''$  (<1%),  $\mu'$  (<3%) and  $\mu''$  (<1%) for the data. A Hewlett Packard HP 8753ES network analyser setup is used to perform the measurements over a wide range of frequencies (10 MHz-6 GHz). The typical dimensions of the toroids are those of APC7 standard (inner diameter = 3.04 mm, outer diameter = 7 mm, length = 2 mm - 4mm). The material has been machined in order to avoid the presence of air gaps between the sample and the line walls. The data were obtained at room temperature.

### FIG. 4 HERE

Figure 4 show the frequency response of the complex permeability of the samples under study. The permeabilities at 100 MHz take close values to those measured at 100 Hz (Tab.1). Therefore the possible contribution of wall displacements can be excluded. A common feature of these spectra is the relative high frequency values at which a peak in  $\mu''$  - corresponding to the dispersion of  $\mu'$  - can be identified. Noteworthy results are presented by sample (a): complex permeability and permittivity show almost constant values in the whole frequency range from 100MHz up to 1GHz ( $\mu=3.5-j0.15$  and  $\epsilon=6-j0.13$ ) that leads to a refractive index  $n=4.85$  (Fig.5). The low value taken by  $\mu''$  is a also good indicator of the absence of wall relaxation at lower frequencies. The values of the loss tangents are moderate (Fig.6):  $\text{tg}\delta_\mu=0.04$  and  $\text{tg}\delta_\epsilon=0.02$ . The resonance frequency is  $f_R=2.34$  GHz. In term of material performances these data compare well, in particular, with recent ones [2], [3],[11], that cover the range 3-30MHz.

### FIG. 5 HERE

### FIG. 6 HERE

It is known that the resonance frequency  $f_r$  and the static permeability  $\mu_{\text{init}}$  are related to each other by well known Snoek's law [12]:  $(\mu_{\text{init}} - 1).f_r = \frac{2}{3}(\gamma.M_S)$  where  $M_S$  is the saturation magnetization, and the gyromagnetic coefficient is  $\gamma = 2.8\text{MHz/Oe}$ . If the porosity is reduced,  $\mu_{\text{init}}$  is expected to increase and  $f_r$  expected to decrease. Here,  $f_r$  may be seen as the permeability cut off frequency. As shown in table 1, samples (a) to (d) follow Snoek's law. Using some other well

known relations:  $f_r = \gamma.H_{\text{eff}}$ ,  $\chi_{\text{init}} = \mu_{\text{init}} - 1 = \frac{2}{3} \frac{M_S}{H_{\text{eff}}}$ , and

$$H_{\text{eff}} = \frac{4}{3} \frac{K}{M_S} \quad (\text{where } H_{\text{eff}} \text{ is the total anisotropy field, } K \text{ is the}$$

total energy of the anisotropy, and  $M_S$  the saturation magnetization) we get from our experiments  $H_{\text{eff}}=69.44$  kA/m,  $M_S=403$  kA/m,  $K=2.62 \cdot 10^4$  J/m<sup>3</sup>. The anisotropy constant  $K$  depends mainly on the magnetocrystalline anisotropy field, and on the shape anisotropy field (that comes from inner demagnetizing effects). No other noticeable contributions to  $K$  (the ratio surface/volume of the grain is high, that excludes surface anisotropy effects [13] ; and the stress due to magnetoelasticity has been relaxed during the heat treatment). A comparison with values for  $\text{Ni}_{0.5}\text{Zn}_{0.5}\text{Fe}_2\text{O}_4$  [14] ( $M_S=450$  kA/m,  $K=0.42 \cdot 10^4$  J/m<sup>3</sup>, ) underlines the contribution due to the substitution by cobalt: the magnetocrystalline anisotropy is strongly increased, that leads  $K$  to increase. Also  $M_S$ , and then  $\chi_{\text{init}}$ , decrease. It has been also demonstrated that magnetic gaps that originate from the porosity, as well as non magnetic grain boundaries, may cause a cut-off in the magnetic flux-paths in the medium, leading to inner demagnetizing effects that increase the magnetic anisotropy and contribute to the shift to higher values of the frequency of spin resonance  $f_R$  [15]-[16]. This phenomenon takes place only below the percolation threshold in magnetic matter (i.e. for porosity higher than 0.35, typically), so that the contribution of demagnetizing effects to the total anisotropy will not be retained in the present study.

The heat treatment submitted to the ferrite powder leads to a porous material with high ferrite content that can be considered to be in the intermediate state between the sintered ferrite and the composite. Then we take advantage of the porous character of the obtained ceramic sample to get ferrite with a noticeable high resonance frequency.

A striking point in the presented data is the low level of magnetic (and dielectric) losses tangents, which clearly distinguish our results.

#### IV. CONCLUSION

Ferrite nanopowder  $\text{Ni}_{0.5}\text{Zn}_{0.3}\text{Co}_{0.2}\text{Fe}_2\text{O}_4$  was synthesized using co-precipitation technique, calcinated, pressed and sintered at temperatures between 850°C to 1000°C. For sample (a) ( $T_S=850^\circ\text{C}$ ) the measured magnetic and dielectric loss tangents show values close to 0.04 and 0.02 respectively in the frequency range from 100 MHz up to 1 GHz. In the same frequency range, we get the following constant values:  $\mu'=3.5$  and  $\epsilon'=6$ , that is a refractive index  $n=4.85$ . This low-temperature sintering material can be considered to be in an intermediate state between the sintered ferrite and the composite. This porous structure of the material- that induced gaps between the magnetic grains- can be invoked to explain the unusual-for spinel ferrites materials- high value of the relaxation phenomenon. These electromagnetic performances fit the requirements for the design of antennas (VHF-UHF range) with reduced size.

#### ACKNOWLEDGMENT

This work was supported in part by the Agence Nationale pour la Recherche (ANR-NAOMI project).

#### REFERENCES

- [1] J. Holopainen, J. Villanen, M. Kyro, C. Icheln; P. Vainikainen, *Antenna Technology Small Antennas and Novel Metamaterials*, IEEE International Workshop, pp.305 – 308, March 6-8, 2006.
- [2] L.B. Kong, Z.W. Li, G.Q. Lin, Y.B. Gan, "Ni-Zn ferrites composites with almost equal values of permeability and permittivity for low-frequency antenna design", *IEEE Trans. Magn.*, vol. 43, pp. 6-10, January 2007; and also: L.B. Kong, Z.W. Li, G.Q. Lin, Y.B. Gan, "Electrical and magnetic properties of magnesium ferrite ceramics doped with BiO<sub>3</sub>", *Acta Materialia*, vol. 55, pp.6561-6572, 2007.
- [3] N. Koga, T. Tsutaoka, *J. Magn.Magn. Mater.* 313, 168-175 (2007).
- [4] S. Sugimoto, K.Haga, T. Kadotani, K. Inomata, *J. Magn.Magn. Mater.*290-291, 1188 (2005).
- [5] P.Mathur, A. Thakur, M.Singh, *J. Magn. Magn. Mater.* 320, 1364-1369 (2008)
- [6] B.D Cullity, *Elements of X-ray diffraction*, Eddison Wesley Reading, M.A., 1978
- [7] P.Mathur, A.Thakur, M.Singh, G. Harris, *Z. Phys.Chem.* 222, 621-633 (2008).
- [8] A. Verma, R. Chatterjee, *J. Magn. Magn. Mater.* 306, 313-320 (2006).
- [9] P.J. Van der Zaag, J.J.M. Ruijgrok, A. Noordermeer, M.H.WM. Van Delden, P.T. Por, M.Th. Rekveldt, D.M. Donnet, J.N. Chapman, "The initial permeability of polycrystalline MnZn ferrites: The influence of domain and microstructure", *J. Applied Phys.*, vol. 74, N° 6, pp.4085-4095, Sept. 1993.
- [10] J. Baker-Jarvis, E. J. Vanzura, W. A. Kissck "Improved technique for determining complex permittivity with the transmission reflexion method" *IEEE Trans. On Micr. Theo. And Tech.*, vol. 38, N°8, august 1990.
- [11] L.Z. Wu, J. Ding, H.B. Jiang, C.P. Neo, L.F. Chen, C.K. Ong, "High frequency complex permeability of iron particles in a non magnetic matrix", *J. Applied Physics*, Vol.99, N°8, p.083905-1- 083905-7, April 2006.
- [12] J-L. Snoek, *Physica*, 14, 207 (1948).
- [13] V.P. Shilov, Y. Raikher, J.-C. Bacri, F. Gazeau, R. Perzynski, "Effect of unidirectional anisotropy on the ferromagnetic resonance in ferrite nanoparticles", *Phys. Rev. B*, vol. 60, pp.11902-11905, November 1999.
- [14] J. Gieraltowski, *Journal de Physique*, C1, Vol.38, C1-57, (1977).
- [15] J.L. Mattei, M. Le Floc'h, "Percolative behavior and demagnetizing effects in disordered heterostructures", *J. Magn. Magn. Mat.*, vol.257, pp.335-345, 2003
- [16] J.L. Mattei, M. Le Floc'h, "Effects of the magnetic dilution on the ferrimagnetic resonance of disordered heterostructures", *J. Magn. Magn. Mat.*, vol. 264, pp.86-94, 2003

Corresponding author: Jean-Luc Mattei (e-mail: mattei@univ-brest.fr)

TABLE 1  
Temperatures of calcination ( $T_c$ ) and sintering ( $T_s$ ), permeability and permittivity of sintered  $Ni_{0.5}Zn_{0.3}Co_{0.2}Fe_2O_4$ . (n.m.: not measured)

Sample label	$T_c$ ( $^{\circ}C$ )	$T_s$ ( $^{\circ}C$ )	density (g/cm <sup>3</sup> )	porosity	$(\mu'-1)$ @10 <sup>2</sup> Hz	$(\mu'-1)$ @100MHz	$f_r$ (GHz)	$(\mu'-1)$ . $f_r$
(a)	800	850	4.15	15%	3.9	2.51	2.41	6.05
(b)	800	900	4.459	7%	n.m.	3.57	1.78	6.35
(c)	800	950	4.518	6%	n.m.	3.95	1.54	6.08
(d)	800	1000	4.740	1%	6.3	4.64	1.36	6.31

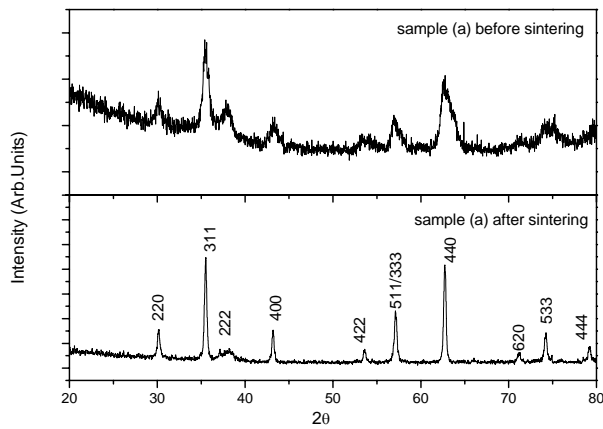


Fig. 1. : XRD of powdered sample of  $Ni_{0.5}Zn_{0.3}Co_{0.2}Fe_2O_4$  ferrite.

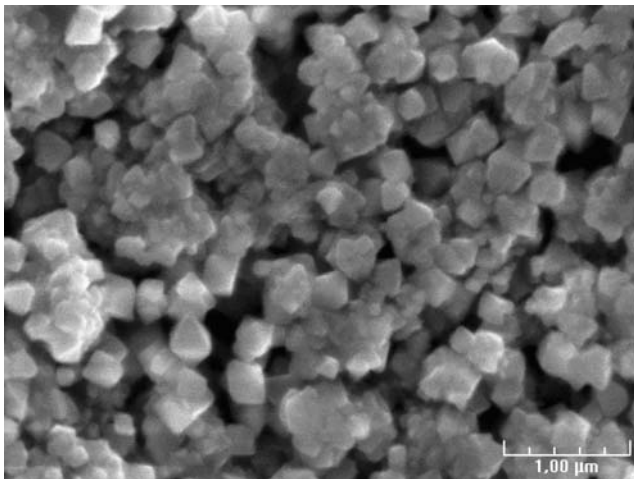


Fig.2 : SEM image of the surface of  $Ni_{0.5}Zn_{0.3}Co_{0.2}Fe_2O_4$  ferrite after heat treatment at 850  $^{\circ}C$ .

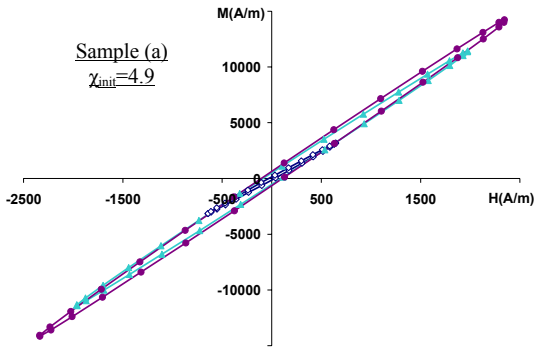


Fig.3a : First magnetization curves for sample (a) (frequency=100Hz).

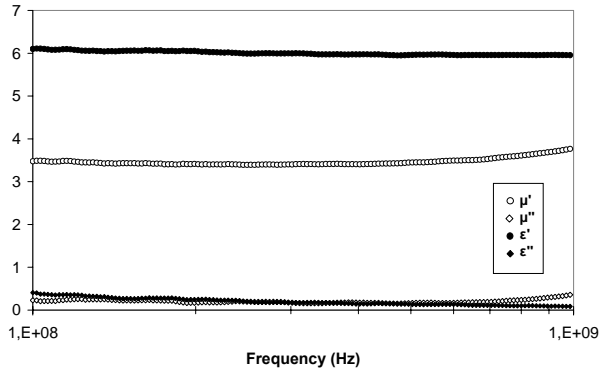


Fig.5 : Measured complex permeability and permittivity spectra of sample (a) between 100 MHz and 1GHz.

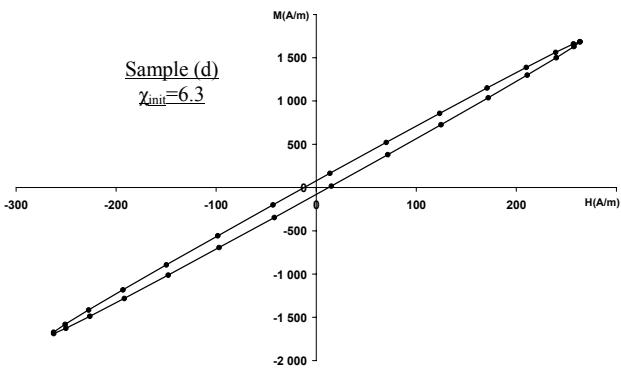


Fig.3b : First magnetization curves for sample (d) (frequency=100Hz).

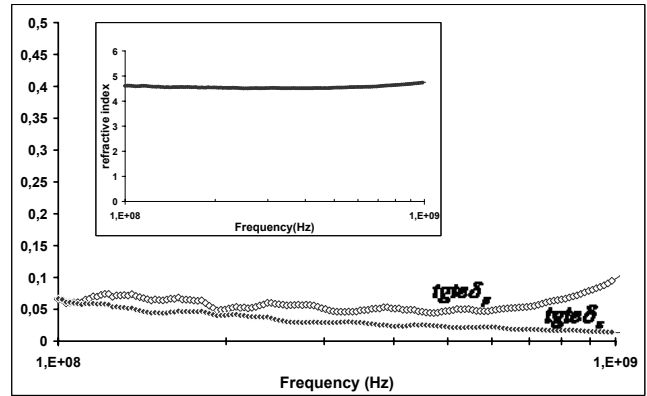


Fig.6 : Loss tangents for sample (a) between 100 MHz and 1GHz. Inset picture depicts refractive index.

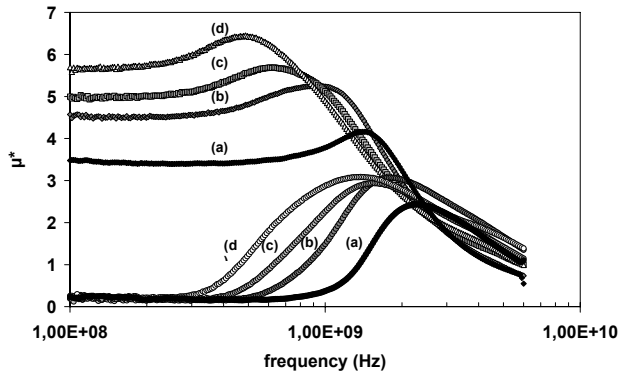


Fig.4 : Real and imaginary parts of permeability for  $Ni_{0.5}Zn_{0.3}Co_{0.2}Fe_2O_4$  ferrites.